Article

Not peer-reviewed version

Application of the Sponge Model Implants in the Study of Vaccine Memory in Mice Previously Immunized with LBSap

Mariana Ferreira Lanna , Lucilene Aparecida Resende * , Paula Mello De Luca , Wanessa Moreira Goes , Maykelin Fuentes Zaldívar , André Tetzl Costa , Walderez Ornelas Dutra , Alexandre Barbosa Reis , Olindo Assis Martins-Filho , Kenneth Jhon Gollob , Sandra Aparecida Lima De Moura , Edelberto Santos Dias , Érika Michalsky Monteiro , Denise Silveira-Lemos , Rodolfo Cordeiro Giunchetti *

Posted Date: 24 October 2024

doi: 10.20944/preprints202410.1748.v1

Keywords: sponge implant model; vaccine; immune response; mice

 doi:10.20944/preprints202410.1748.v1

Article

Application of the Sponge Model Implants in the Study of Vaccine Memory in Mice Previously Immunized with LBSap

Mariana Ferreira Lanna [1,2,†], Lucilene Aparecida Resende [2†], Paula Mello De Luca [3], Wanessa Moreira Goes [1], Maykelin Fuentes Zaldívar [1], André Tetzl Costa [1], Walderez Ornelas Dutra [1], Alexandre Barbosa Reis [2], Olindo Assis Martins-Filho [4], Kenneth Jhon Gollob [5], Sandra Aparecida Lima de Moura [6], Edelberto Santos Dias [7], Érika Michalsky Monteiro [7], Denise Silveira-Lemos [1,8] and Rodolfo Cordeiro Giunchetti [1*]

1 Laboratory of Biology of Cellular Interactions, Department of Morphology, Federal University of Minas Gerais, Belo Horizonte, Minas Gerais, Brazil
2 Immunopathology Laboratory, Biological Sciences Research Center/NUPEB, Institute of Exact and Biological Sciences, Federal University of Ouro Preto, Ouro Preto, Minas Gerais, Brazil
3 Instituto Oswaldo Cruz (IOC), FIOCRUZ Av. Brasil, Rio de Janeiro 21040-900, Brazil
4 Integrated Biomarker Research Group, René Rachou Research Institute, Oswaldo Cruz Foundation, Belo Horizonte, Minas Gerais, Brazil
5 Albert Einstein Israeli Institute of Education and Research. Albert Einstein Hospital. São Paulo. São Paulo, Brazil
6 Biomaterials and Experimental Pathology Laboratory, Institute of Exact and Biological Sciences, Federal University of Ouro Preto, Ouro Preto, Minas Gerais, Brazil
7 Taxonomy of Phlebotomines/Epidemiology, Diagnosis and Control of Leishmaniasis Group, René Rachou Research Institute, Oswaldo Cruz Foundation, Belo Horizonte, Minas Gerais, Brazil
8 José Rosário Vellano University, Belo Horizonte, Minas Gerais, Brazil
* Correspondence: giunchetti@icb.ufmg.br
† These authors contributed equally to this work.

Abstract: Considering the large number of candidates in vaccine testing studies against different pathogens and the amount of time spent in the pre- and clinical trials, there is a pressing need to develop an improved *in vivo* system to quickly screen vaccine candidates. The model of a polyester-polyurethane sponge implant provides a rapid analysis of the specific stimulus-response, allowing the study of a compartmentalized microenvironment. The sponge implant's defined measurements were standardized as a compartment to assess the immune response triggered by vaccinal antigen. The LBSap vaccine (composed by *Leishmania braziliensis* antigens associated with saponin adjuvant) was used in the sponge model to assess the antigen-specific immunological biomarker, including memory generation after initial contact with the antigen. Mice strains (Swiss, BALB/c, and C57BL/6) were previously immunized using LBSap vaccine followed by an antigenic booster performed inside the sponge implant. The sponge implants were assessed after 72 hours, and the immune response pattern was analyzed according to leukocyte immunophenotyping and cytokine production. After LBSap vaccination, the innate immune response of the antigenic booster in the sponge implants demonstrated higher levels in the Ly+ neutrophils and CD11c+ dendritic cells with reduced numbers of F4/80+ macrophages. Moreover, the adaptive immune response in Swiss mice demonstrated a high CD3+CD4+ T-cells frequency consisting of an effector memory component in addition to a cytoxicity response (CD3+CD8+ T-cells), displaying the central memory biomarker. The major cell surface biomarker in the BALB/c mice strain was related to CD3+CD4+ effector memory while the increased CD3+CD8+ effector memory was highlighted in C57/BL6. The cytokine profile was more inflammatory in Swiss mice, with the highest levels of IL-6, TNF, IFN-g, and IL-17, while the same cytokine was observed in in C57BL/6 yet modulated by enhanced IL-10 levels. Similar to Swiss mice, BALB/c mice triggered an inflammatory environment after the antigenic booster in the sponge implant with the increased levels in the ILL-6, TNF, and IFN-g. The results highlighted how genetic background can influence populations involved in the immune response and indicated that it is possible to use this model to optimize and monitor the innate and adaptive immune responses of vaccine candidates. In this sense, these results could guide the choice of the most appropriate experimental model in

 doi:10.20944/preprints202410.1748.v1

biomolecule tests, considering that the particularities of each mouse strain influenced the dynamics of the immune response.

Keywords: sponge implant model; vaccine; immune response; mice

1. Introduction

The sponge implant has been applied as an important *in vivo* model for the study of angiogenesis and inflammatory processes [1–4]. After implantation in the subcutaneous compartment, the acellular and avascular sponge matrix induces the migration, proliferation, and accumulation of inflammatory cells, angiogenesis, and extracellular matrix deposition in its trabeculae [1,5]. The sponge implant model allows the sequential study of the inflammatory infiltrate through histomorphometric and biochemical analyses, using the activity of the enzymes and myeloperoxidase (MPO) and N-acetyl-glucosaminidase (NAG) to indirectly determine the activation of neutrophils and macrophages [4,6–8]. Furthermore, since the tissue reaction to the sponge implant is circumscribed by a connective tissue capsule, it is also possible to assess the chemokine and cytokine profile in this microenvironment [4,5,9–11].

Notably, the sponge implant can be used to analyze the immune response in a controlled microenvironment, which represents a preliminary step in the development of an *in vivo* platform to test potential biomolecules. Many studies investigate this compartmentalized microenvironment in response to implant-associated anti-inflammatory or anti-angiogenic molecules [2,5,10,12–23]. The characterization of the immune events, including leukocyte immunophenotyping, cell activation, and the cytokine profile in sponge implanted in mice (Swiss, BALB/c and C57BL/6), demonstrated the influence of the genetic background with the inflammatory kinetics [11]. The appropriate time-points after the implant sponge as the platform of biomolecules screening was described according to the mice background: Day5 post-implant for Swiss mice, Day7 for BALB/c mice, and Day6 for C57BL/6 mice. Those time-points disclosed minor inflammation triggered by the sponge that induced an expected foreign body reaction post-implant [11]. Among the possible applications of studies using the sponge implant as a model, we highlight the possibility of trialing antigen candidates to compose protective vaccine formulations.

In this context, our group has described the ability of LBSap vaccine (composed by *Leishmania braziliensis* antigens associated with saponin adjuvant) to trigger a protective immune response in mice, hamsters, and dogs [24–35]. These studies supported the LBSap vaccine as a formulation presenting protective antigens useful for validating the sponge implant as model for memory immune response analyses. This new *in vivo* compartmentalized platform could be employed to optimize the screening of potential antigens required in protective vaccines. Thus, this study aimed to evaluate the sponge implant model in a vaccine memory test using the LBSap vaccine as a reference to improve the understanding of vaccine immunogenicity to establish a new model for *in vivo* tests. For this purpose, the immune response was further characterized using a prime (vaccine) and boost (antigen inoculation at sponge implant) protocol.

2. Materials and Methods

2.1. Animals

Male Swiss, BALB/c, and C57BL/6 mice (8–10 weeks old; n=20 mice) were provided by the Centro de Ciência Animal (CCA) at Universidade Federal de Ouro Preto (UFOP), Brazil. The animals were kept in ventilated racks with food and water ad libitum throughout the study, with intermittent light/dark cycles every 12 hours. The experimental design was approved by the Ethical Committee for Animal Studies (CEUA/UFOP, # 014/2011).

2.2. Sponge Implants

 doi:10.20944/preprints202410.1748.v1

All the procedures were performed as described by [11]. Briefly, disk-shaped (5mmx8mm) polyether-polyurethane sponges were soaked overnight in 70% v/v ethanol and boiled in distilled water for 15 min before implantation. The mice were anesthetized by intraperitoneal injection of ketamine (150 mg kg−1) plus xylazine (10 mg kg−1) and the dorsal fur was shaved and the skin wiped with 70% v/v ethanol. The sponge disks were subcutaneously implanted throughout a 1-cm long dorsal mid-line incision and the animals were monitored daily for discomfort /distress or signs of opportunistic infection.

2.3. Experimental Design

The dynamics of phenotypic and functional changes in the sponge microenvironment were previously reported [11] to support the selection of the best post-implantation time, since this information is crucial for use in biomolecule screening assays. Therefore, Day 5/Swiss, Day 7/BALB/c, and Day 6/C57BL/6 were chosen for an immunological memory study [11]. The sponge model was applied to the investigation of vaccine memory in previously immunized animals. The experimental design, study groups, and timeline are provided in Figure 1.

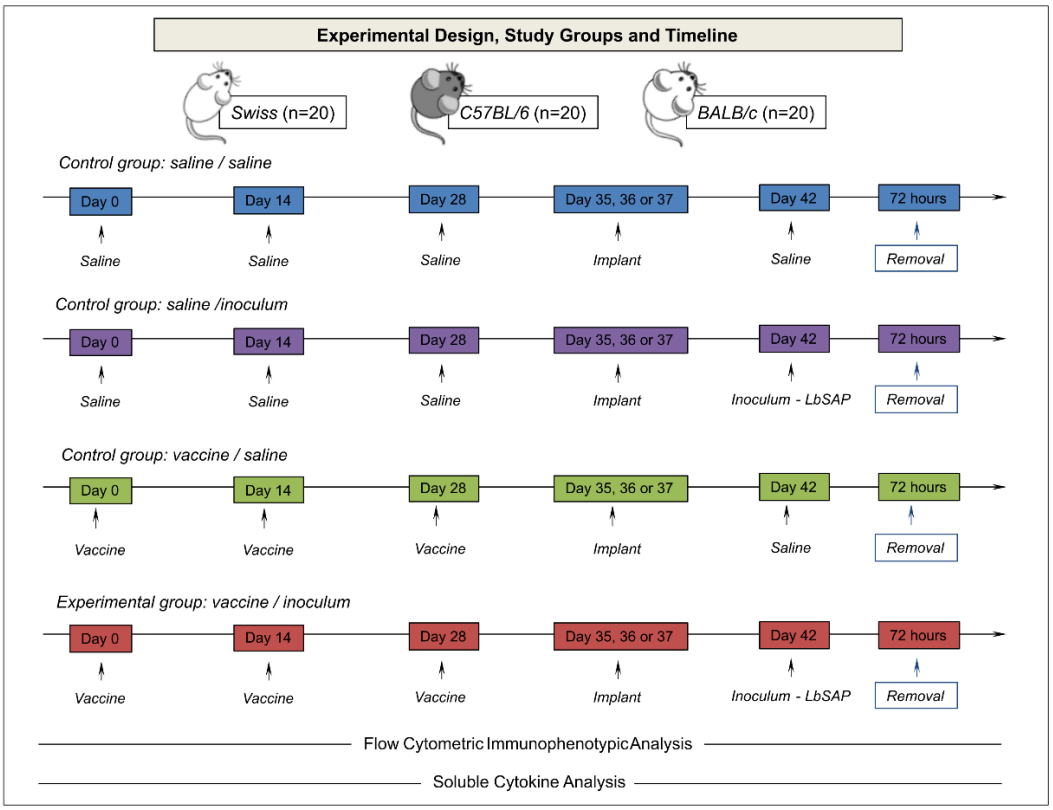

Figure 1. Experimental design and study groups. The animals were divided into three control groups and one experimental group, and submitted to inoculation with saline or vaccine, subcutaneously, and saline or inoculum with *L. braziliensis* vaccine antigen (without the adjuvant) in the sponge, on the days listed. The implanted sponge discs were removed and sent for immunophenotyping analysis by flow cytometry and for investigation of soluble cytokines.

The animals were divided into three control groups (Figure 1): Saline/Saline (S/S): consisted of three saline inoculums, subcutaneously, with a 14-day interval and a new saline inoculum performed inside the sponge implant 14 days after the last inoculum; Saline/Inoculum (S/I): consisted of three saline inoculums, subcutaneously, at 14-day intervals and a new inoculum performed 14 days after the last inoculum in the sponge implant with 60 µg of *Leishmania braziliensis* antigen (produced as described by Giunchetti et al. [28]); Vaccine/Saline (V/S): consisted of three inoculums of LBSap vaccine (60 µg of *Leishmania braziliensis* antigen and 50 µg saponin per dose - produced as described

 doi:10.20944/preprints202410.1748.v1

by Giunchetti et al. [28]), subcutaneously, with a 14-day interval; a new inoculum was performed 14 days after the last inoculum in the sponge implant with saline; and an experimental group Vaccine/Inoculum (V/I): consisted of three inoculums of the LBSap vaccine (60 μg of *Leishmania braziliensis* antigen and 50 μg saponin per dose), subcutaneously, at 14-day interval and a new inoculum performed 14 days after the last inoculum on the sponge implant with 60 μg of *Leishmania braziliensis* antigen. After 72 hours of the different inoculum in the sponge implants, the animals were euthanized, and the sponges were removed for immunophenotypic analysis and soluble cytokine measurements.

2.4. Flow Cytometry Immunophenotyping

The leukocyte subsets were harvested from sponge implants and analyzed by flow cytometry as previously described Lanna et al.[11]. A panel of fluorescent monoclonal antibodies were used, including anti-CD45 (APC clone 30-F11/E071491630, FITC clone Sa230-F11/E003051630), anti-CD3 (Pe-Cy5 clone 145-2C11/E060661630), anti-CD8 (APC clone 53.6-7/E070561330), anti-CD11c (Pe-Cy5 clone N418/E006121631), F4/80 (FITC clone BM8/E006121631), LY6G (APC clone RB6-8C5/ E001610630), anti-CD197 (PerCPCy5.5 clone 4B12/E0800369258) and anti-CD62L (Pe clone MEL-14/E009159357) from e-Bioscience (San Diego, CA, USA), and anti-CD4 (FITC clone RM4-5/714474A) from Invitrogen (Carlsbad, CA, USA).

The sponges were removed from the implant site and incubated for one hour in a solution containing trypsin, after which the sponge implants were gently squeezed at room temperature in 2mL of RPMI, and the sponge debris was removed by differential centrifugation at 200Xg for 5 minutes at 4ºC. The supernatant was centrifuged at 400xg for 8 minutes at 4ºC to obtain the cell pellet. After resuspension of the cell pellet, the erythrocytes were lysed using 10mL of ammonium chloride buffer. The leukocytes were washed once with 10mL of RPMI at 400xg for 8 minutes at 4ºC. The cell counts were determined with a Neubauer chamber, and the final cell suspension was adjusted to $1x10^5$ cells/mL. Aliquots of 100μL of cell suspension (e.g.,$1x10^4$ cells per tube) were incubated in polypropylene tubes containing combinations of 20μL of monoclonal antibody. Following incubation, stained cells were washed once with phosphate-buffered saline (PBS) and resuspended in 250μL of PBS. Nonspecific binding was monitored by using fluorochrome-labeled isotypic matched reagents to provide valid negative controls. Autofluorescence was monitored using a negative control in which the cell suspension was incubated in the absence of fluorochrome-labeled monoclonal antibodies but in the presence of dilution and wash buffers. Flow cytometric measurements were performed on a FACSCanto II® instrument (Becton Dickinson, Mountain View, CA). A total of 20,000 events were acquired for each sample. The CELLQuestPro software (Franklin Lakes, NJ) was used for data acquisition and storage. FlowJo Software (Flow Cytometry Analysis Software Version 10.1, Tree Star, Inc., Ashland, OR) was used for data analyses.

2.5. Soluble Cytokine Measurements

The sponge implants were homogenized in 1mL of RPMI using a tissue homogenizer (Homo mix). The homogenates were centrifuged at 3,000xg for 10 min at 4ºC and the supernatants were stored at -80ºC until processing. Soluble cytokine levels were measured by Cytometric Bead Array (BD Biosciences, San Jose, CA, USA), according to the manufacturer's recommendations. The mouse inflammation kit was used to measure the levels of soluble IL-6, IL-10, IL-17, IFN-γ, and TNF. FCAP software v.1.0.2 (BD Biosciences) was used for data analysis. The results were presented in median fluorescent intensity (MFI) values.

2.6. Statistical Analysis

Intragroup and intergroup comparative analysis were performed by One-way ANOVA followed by Tukey's multiple comparison test to compare all pairs of data. In all cases, significance was considered at $p<0.05$. GraphPad Prism (version 5.03, San Diego, California, USA) was used for statistical analysis and graphic arts.

 doi:10.20944/preprints202410.1748.v1

2.7. Biomarker Signature Analysis

The biomarker signature analysis was performed based on the method published by Luiza-Silva et al. which highlights cytokine signatures in innate and adaptive immunity after yellow fever vaccination [36]. This method allows the identification of subtle differences that are not usually detectable by conventional statistical approaches but are relevant for understanding the complex immunological microenvironments that involve multiple events. Biomarker signatures were determined by the frequency of the proportion of implants with biomarker levels above the global median cut-off defined for each biomarker. Thus, to detect the global median cutoff point, the data set was listed in numerical order, from lowest to highest value, after which the median was calculated for each subset of cells (CD45+, Ly+, F4/ 80+, CD11c+, CD3+CD4+, CD3+D8+, CD62L+CCR7+, and CD62L-CCR7-) and each soluble cytokine (IL-6, TNF, IFN-γ, IL-10, and IL-17), using Microsoft Excel software. This approach was performed using all the data for each of the indicated biomarkers, including the data relating to all experimental groups (S/S, S/I, V/S, and V/I) and all three strains of mice (Swiss, BALB/c, and C57BL/6). Based on the global median cutoff, results were categorized as "low" (below the global median) or "high" (above the global median). The categorical data were then used to calculate the proportion (percentage) of implants with biomarker levels above the global median. The curve comprising the ascending frequencies of the biomarkers was created for each experimental group. Biomarkers with frequencies above 75% were considered relevant and highlighted in bold underlined format. Microsoft Excel software was used to assemble radar charts and the final artwork.

3. Results

The data from innate immune response, including the population of total CD45+ leukocytes (LEU) and dendritic cells (CD11c+), macrophages (F4/80+), and neutrophils, (Ly+) are described in Figure 2.

 doi:10.20944/preprints202410.1748.v1

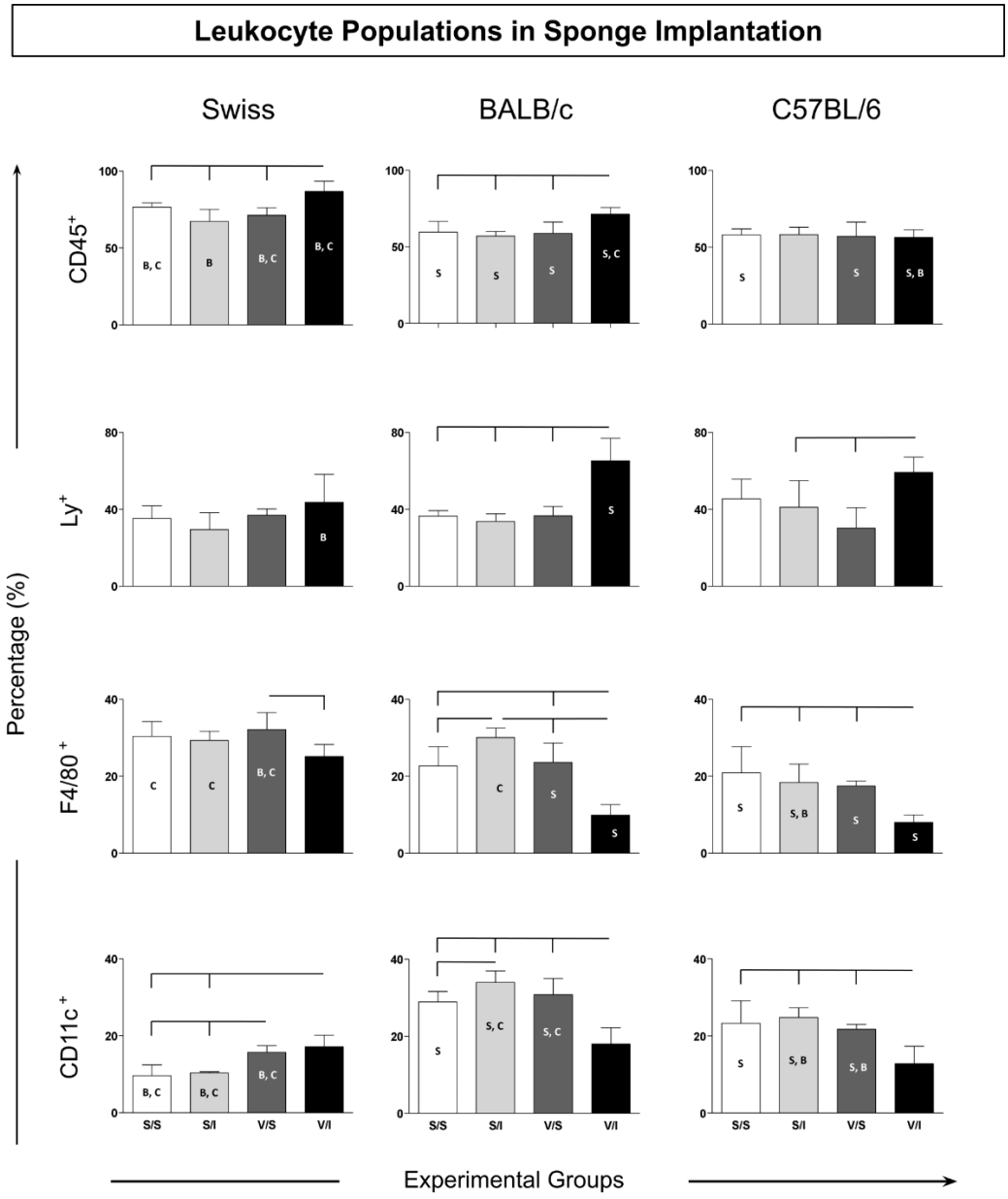

Figure 2. Immunophenotypic profile of leukocytes in sponge implants. The cellular infiltrate removed from the implants was labeled with a monoclonal antibody for quantification by flow cytometry of leukocyte subpopulations (CD45+) of innate immunity cells: neutrophils (LY+), macrophages (F4/80+) and dendritic cells (CD11c+). Data were reported as mean percentage ± standard deviation. Intragroup and intergroup comparisons were evaluated and significant differences ($p < 0.05$) were highlighted by connecting lines within the lineage and by the letters "S", "B" and "C" for comparisons between Swiss, BALB/c mice or C57BL/6, respectively.

An increase in total CD45+ leukocytes in Swiss mice was observed in the experimental group (V/I) as compared to the other groups (S/S, S/I, and V/S) and BALB/c (S/S and S/I) mice (Figure 2 – upper panel). When the strains were compared, a higher percentage of CD45+ leukocytes were highlighted in Swiss followed by BALB/c and C57BL/6 mice. Regarding the Ly+ neutrophils, an increase was observed in the V/I group of BALB/c mice as compared to the other groups (S/S, S/I, and V/S) (Figure 2 – middle panel). Similarly, the C57BL/6 mice demonstrated higher Ly+ neutrophils in the V/I group as compared to the S/I and V/S groups (Figure 2 – middle panel). Interestingly, Swiss mice had a lower percentage of Ly+ neutrophils in the V/I group as compared to BALB/c mice. F4/80+ macrophages showed a heterogeneous distribution between the experimental groups, but the

 doi:10.20944/preprints202410.1748.v1

percentage in all strains was lower in the V/I group as compared to the other groups (Figure 2 – middle panel). When studying CD11c+ dendritic cells in Swiss mice, an increase was reported in the V/S and V/I groups as compared to the other groups (SS/ and S/I) (Figure 2 – bottom panel). In contrast, there were a decrease in the percentage of dendritic cells CD11c+ in the V/I group in BALB/c and C57BL/6 mice in relation to the other groups (S/S, S/I, and V/I).

The adaptive immune response cells were evaluated according to total T-cells (CD3+) and their T-cells subsets (CD3+CD4+ and CD3+CD8+). Also analyzed in those T-cells subsets were the immunological memory biomarkers: CD62L+CCR7+ (central memory) and CD62L-CCR7- (effector memory) (Figure 3). The data described a similar pattern of CD3+CD4+ T-cells in Swiss and C57BL/6 mice with increased counts in the V/I group as compared to the other experimental groups (S/S, S/I, and V/S) (Figure 3 – upper panel). In contrast, the BALB/c mice presented the lowest levels in the CD4+ T-cells in the V/I group as compared to the other two mice strains (Swiss and C57/BL6) (Figure 3). Despite the effector memory (EM) CD4+ T-cells, the Swiss mice presented enhanced levels in the V/S and V/I groups as compared to the S/S group (Figure 3 – middle panel). Similar results were observed in the BALB/c mice, showing higher counts of EM CD4+ T-cells in the V/I group as compared to the S/I group. However, in the C57BL/6, all analyzed groups displayed almost one hundred percent of the CD4+ T-cells EM.

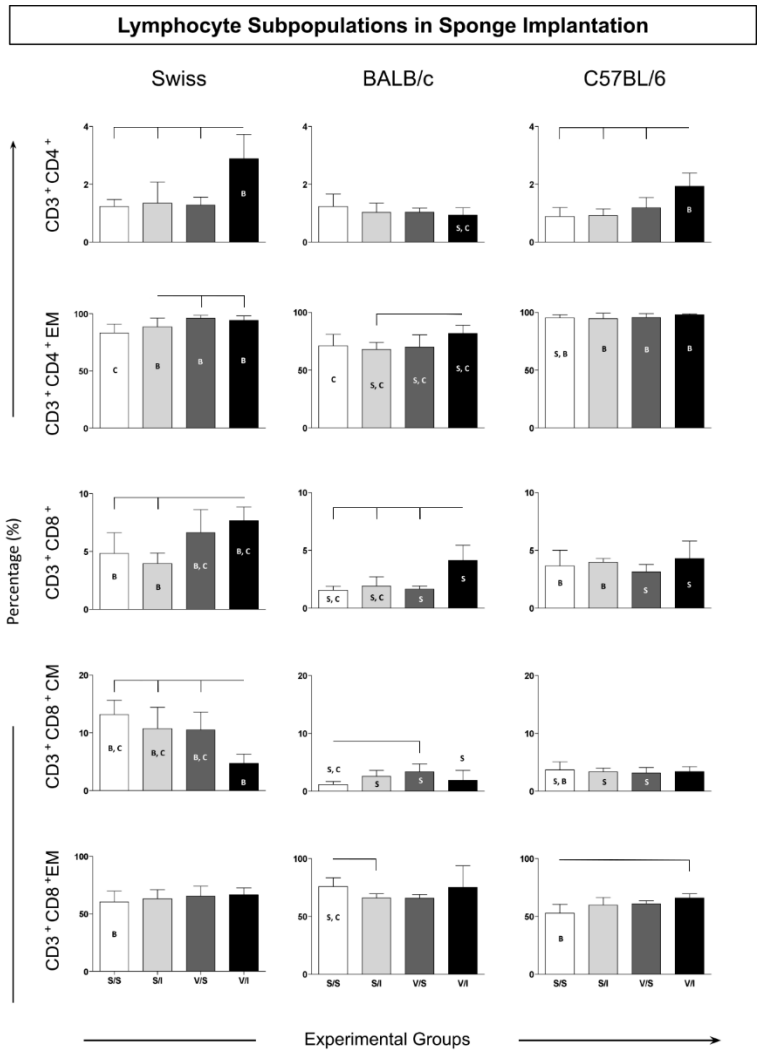

Figure 3. Immunophenotypic profile of lymphocytes in sponge implants. The cellular infiltrate was quantified by flow cytometry for the TCD3+ CD4+ and TCD3+ CD8+ lymphocyte subpopulations, in addition to the EM effector memory (CD62L+CCR7+) and CM central (CD62L+CCR7+) subpopulations. Data were reported as mean percentage ± standard deviation. Intragroup and intergroup comparisons were evaluated and significant differences ($p < 0.05$) were highlighted by

 doi:10.20944/preprints202410.1748.v1

connecting lines within the lineage and by the letters “S”, “B” and “C” for comparisons between Swiss, BALB/c mice or C57BL/6, respectively.

The CD8+ T-cell frequency in Swiss mice showed increased levels in the V/I group as compared to the S/S and S/I groups (Figure 3 – middle panel). The V/I group in BALB/c mice also exhibited an increase as compared to the other three groups (S/S, S/I, and V/S). Although no changes had been observed in the groups of the C57BL/6 mice, the levels of CD3+CD8+ T-cells were the highest in the groups V/S and V/I of Swiss mice as compared to the same groups from BALB/c and C57/BL6. The central memory (CM) CD8+ T-cells in Swiss mice showed lower levels in the V/I group as compared to the other experimental groups (Figure 3 – middle panel). While there was no change in the CM CD8+ T-cells between the groups of C57BL/6 mice, enhanced counts were observed in the V/S group of BALB/c mice as compared to the S/S group. The Swiss mice presented the highest levels of CM CD8+ T-cells in relation to the other mice strains. Concerning effector memory (EM) CD8+ T-cells, the BALB/C mice displayed a decrease in the S/I group as compared to the S/S group, whereas in C57BL/6 mice, the V/I group showed higher levels of this cell population as compared to the S/S group (Figure 3 – bottom panel).

3.2. Cytokine Microenvironment in the Sponge Implants

The cytokine microenvironment in the sponge implants was analyzed to determine the amounts of soluble cytokines (IL-6, TNF, IFN-γ, IL-10, and IL-17). This panel of cytokines was chosen to evaluate the induction of a microenvironment related to an inflammatory or immunomodulatory profile in the microenvironment of the sponge implant. The soluble cytokines in the sponge implant for Swiss, BALB/c, and C57/BL6 mice strains showed higher IL-6 levels in the V/I group as compared to the S/I and V/S groups (Figure 4 – upper panel). There was also an increase in TNF levels in the V/I groups considering all mice strains when compared to the other experimental groups.

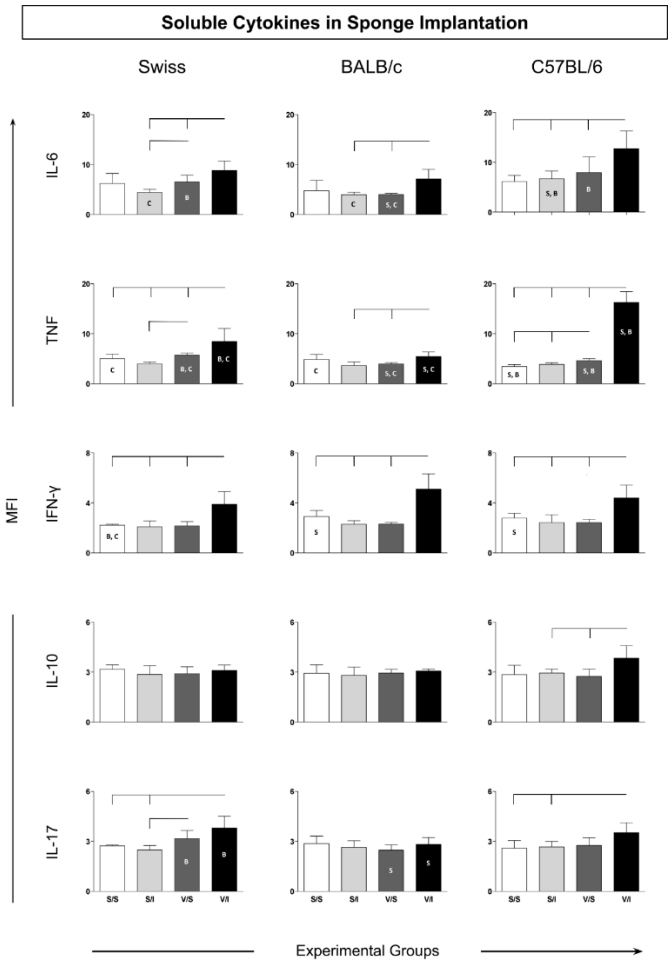

 doi:10.20944/preprints202410.1748.v1

Figure 4. Soluble cytokines in the microenvironment of sponge implants. Data are reported as mean percentage and standard deviation of mean fluorescence intensity (MFI) for each cytokine (IL-6, TNF, IFN-γ, IL-10, IL-17). Significant differences ($p < 0.05$) are represented by the connecting lines above the graphs (differences considering the same lineage, but different groups), and by the letters "S", "B" and "C", considering the differences in the same group in different strains of Swiss, BALB/c or C57BL/6 mice, respectively.

Notably, the V/I group in C57BL/6 mice displayed the highest IL-6 levels as compared to Swiss and BALB/c mice strains. Similarly, an increase in IFN-γ levels in all the mice strains was observed for V/I group as compared to the other three experimental groups (S/S, S/I, and V/S) (Figure 4 – middle panel). The IL-10 cytokine analysis revealed increased levels in C57BL/6 mice considering the V/I group as compared to the S/I group (Figure 4 – middle panel). Similar to other inflammatory cytokines, the IL-17 profile demonstrated higher levels in both Swiss and C57BL/6 mice in the V/I group as compared to S/S and S/I groups without changes in the groups of BALB/c mice (Figure 4 – bottom panel).

3.3. Ascendant Biomarker Signature Implants

To characterize the immunophenotypic and functional profile of the immune response in the sponge among the different experimental groups, the ascendant biomarker signatures (from the lowest to the highest frequency) were assembled as shown in Figure 5. Data analysis confirmed most findings detected by conventional statistical methods. The ascendant biomarker signature in sponge implants involves two sets of data referred to as Leukocytes (LEU) Subsets and Cytokine Production.

Preprints.org (www.preprints.org) | NOT PEER-REVIEWED | Posted: 24 October 2024 doi:10.20944/preprints202410.1748.v1

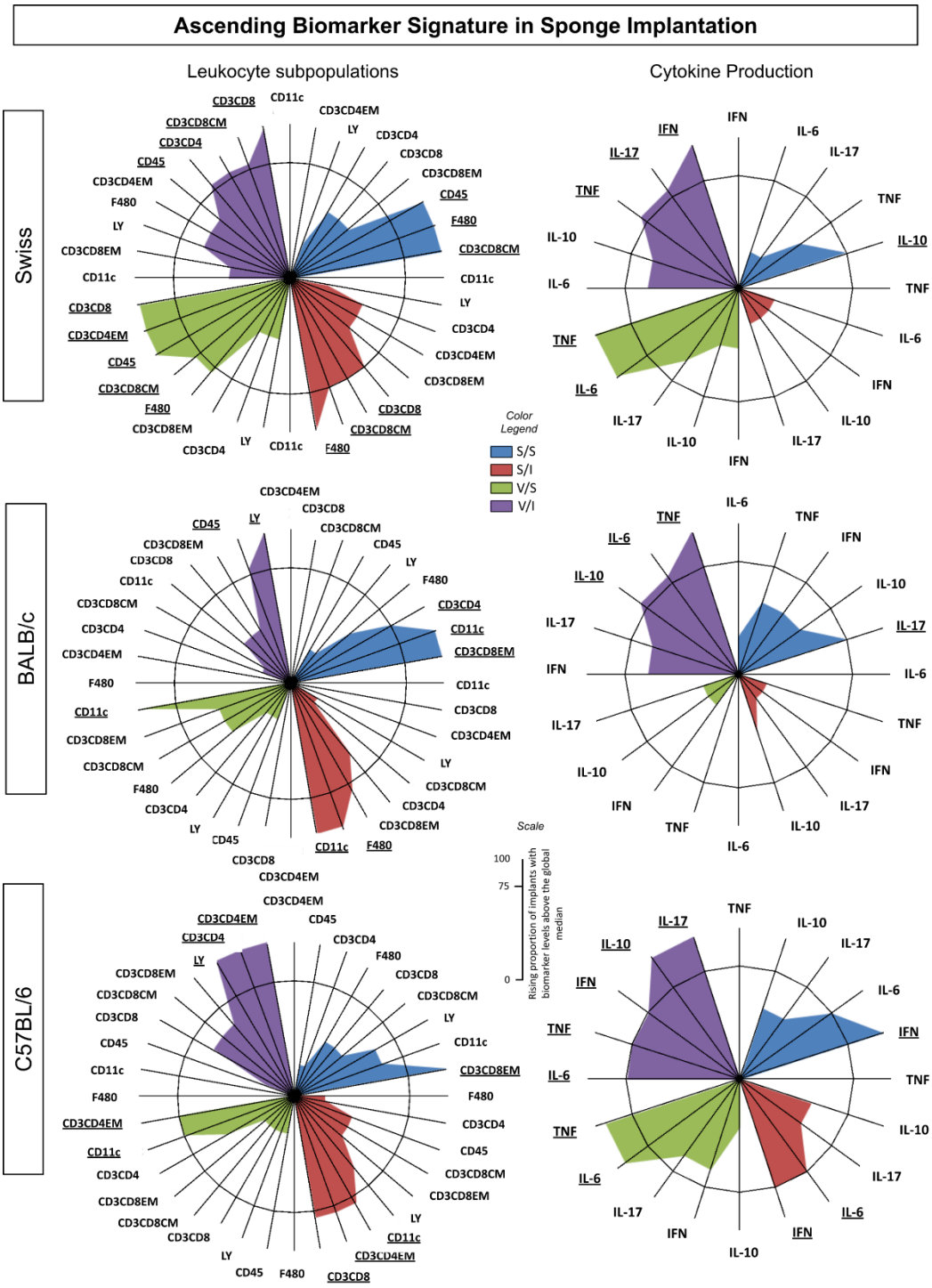

Figure 5. Ascending biomarker signature in sponge implants. Signatures were determined using the frequency of the biomarker level above the global median cutoff defined for each biomarker. Radar plots were used to compile and summarize the ascending proportion of implants with biomarker levels above the global median for each cell subset (CD45+, Ly+, F4/80+, CD11c+, CD3+CD4+, CD3+CD4+ EM, CD3+ CD8+, CD3+CD8+CM and CD3+CD8+ EM), as well as each soluble cytokine (IL-6, TNF, IFN-γ, IL-10 and IL-17), in the different experimental groups [S/S (blue), S/I (red), V/I (green), and V/I (purple)] for Swiss, BALB/c, and C57BL/6 mice. Biomarkers with frequencies equal to or above 75% were considered relevant and highlighted in bold underlined format.

The biomarker signatures of LEU subsets showed that Swiss mice presented the most prominent immune response to the sponge implant, the vaccine, and the inoculum (Figure 5). The Swiss mice

 doi:10.20944/preprints202410.1748.v1

strain displayed higher numbers of cell surface biomarkers with increased levels in all four groups with the recruitment of cytotoxic and central memory immune responses (Figure 5 – upper panel). Moreover, the Swiss mice strain showed an intense inflammatory profile since the highest frequency for TNF, IL-17, and IFN-g was not modulated by IL-10. In contrast, BALB/c mice presented a lower number of cell surface biomarkers with increased levels and a cytokine environment composed of inflammatory cytokines (TNF and IL-6) modulated by IL-10 (Figure 5 – middle panel). Furthermore, the C57BL/6 mice highlighted the T Helper cell surface biomarker with the effector memory component displaying a prominent inflammatory environment with highest frequency of IL-6, TNF, IFN-γ modulated by IL-10 (Figure 5 – bottom panel).

4. Discussion

The sponge model has been widely studied over the past three decades [2,5,8,9,12,14,17,18,37–44], including the phenotypic and functional changes that are triggered in distinct mouse lineages [11]. However, the use of this model for trialing antigen candidates for vaccine formulation has not yet been explored as a tool for determining the immunogenicity profile. The present study aimed to evaluate the sponge implant model for improving the understanding of immunogenicity to establish a new model of antigen *in vivo* testing. The time points for the immune response analysis in the sponge implants were chosen based on the data previously presented for each mouse strain [11].

This study described the changes that vaccination and/or antigen inoculation inside the sponge induced in the total leucocytes (CD45+), in the distinct leukocyte subsets harvested from the sponge, in addition to the cytokine environment. The findings showed an increase in the levels of CD45+ leukocytes in the prime-boost protocol (related to group V/I) in two (Swiss and BALB/c) of the mice strains. In Swiss mice, the higher CD45+ leukocyte counts could be explained by the increase in CD11c+ dendritic cells and in T-cells subsets (CD3+CD4+ and CD3+CD8+). Surprisingly, the vaccination in BALB/c and C57BL/6 mice followed by an antigenic boost in the sponge implant (group V/I) showed an increase in the Ly+ neutrophils, while exhibiting a reduction in the levels of CD11+ dendritic cells and F4/80+ macrophages. Furthermore, the increase in Ly+ neutrophils could partially explain the higher percentage of leukocytes in BALB/c. Interestingly, Mendonça et al. observed a reduction in the frequency of neutrophils when analyzing peripheral blood in BALB/c mice 15 days after LBSap vaccination [24]. These results could indicate the migration of neutrophils to the inflammation (vaccine) site triggered in BALB/c mice. Those results highlighted how the genetic background could influence the immune response triggered by prime (vaccine) and boost (antigen inoculation at sponge implant) protocol. The analysis of F4/80+ macrophages demonstrated a similar pattern of cell infiltration since the percentage of these cells in all mice strains was lower as a result of prime-boost protocol (group V/I). In addition, in BALB/c and C57BL/6 mice, the decreased levels of CD11+ dendritic cells after prime-boost protocol (group V/I) could be explained by the migration to lymphoid organs, such as lymph nodes, for antigen presentation [45]. It is important to emphasize that in BALB/c mice, an increase in both F4/80+ macrophages and CD11+ dendritic cells were observed in the S/I group. It is possible to hypothesize that the type of inoculum (presence of the antigen), without prior vaccination, could temporally trigger this stimulus since both cell types are specialized in antigen presentation.

An investigation of the adaptive immune response showed that the prime-boost protocol was enough to stimulate the selective migration of CD3+CD4+ T-cells in Swiss and C57BL/6, but not in BALB/c mice. It is important to emphasize that the induction of an increase in the amount of CD3+CD4+ T-cells by anti-visceral leishmaniasis vaccines has been associated with high levels of protection due to the ability of these lymphocytes to produce IFN-γ and promote the activation of macrophages favoring leishmanicidal activity [46]. In contrast, a higher count of CD3+CD8+ T-cells was elicited in the BALB/c mice but at a lower level as compared to Swiss mice (V/I group). The previous vaccination of Swiss mice was effective in increasing the levels of CD3+CD8+ T-cells, while the association with the boost (antigen inoculum in the sponge) was required in BALB/c for the expansion of this T-cell subset. Additionally, it has been reported that the LBSap immunization is able to induce enhanced frequency in the circulating T-cells, including their subsets (CD4+ and CD8+)

 doi:10.20944/preprints202410.1748.v1

[28]. Notably, the levels of CD4+ and CD8+ T-cells remained high after *L. infantum* experimental challenge and it was associated with the protection profile [31].

The innate and adaptive immune responses may be related to activation events and maintenance of a protective response profile after vaccination. However, the adaptive response allows the host to trigger an immune memory response, which is of paramount importance in an effective response against pathogens [47,48]. The expansion phase and effector phase of the immune response are followed by an apoptosis phase, during which most antigen-specific T-cells perish. The final phase, or memory phase, is characterized by the maintenance of long-term memory T-cells that retain their antigen specificity and can maintain themselves throughout the life of the host [49,50]. Notably, the most important attribute of a memory immune response compared to a primary immune response is its ability to rapidly generate greater numbers of antigen-specific helper T-lymphocytes and cytotoxic agents. Memory T-cells do not prevent reinfection or recurrence of the disease, but they respond quickly and effectively in this scenario, which is one of the bases for the success of several vaccines [45,47]. Memory T-cells can be classified according to their migratory potential, their ability to proliferate, and produce cytokines [51,52]. Briefly, effector memory (EM) T-cells (CD62L-CCR7-) are present in non-lymphoid peripheral tissues and also circulate in the blood. They can migrate through tissues in search of a particular antigen, where they quickly exert effector functions, such as IFN production and cytotoxic activity [50,51]. However, despite existing in large numbers, effector memory T-cells do not have proliferative potential. Thus, a second line of defense is constituted by central memory (CM) cells (CD62L+CCR7+), which reside and circulate among the secondary lymphoid organs. These cells are type 2 interleukin producers and are very sensitive to antigenic stimulation, capable of rapid proliferation [45].

In summary, EM T-cells provide protection against reinfection or disease reactivation at infection sites, whereas CM T-cells primarily reside in the lymphoid tissue where they rapidly expand and differentiate to replenish the population of effector T-cells. The results of this study demonstrated that Swiss mice are able to trigger an immune response after prime-boost (V/I group) using *Leishmania* antigens marked by (i) increased CD3+CD4+ T-cells and (ii) CD3+CD8+ T-cells with (iii) effector memory based on CD3+CD4+. In BALB/c mice, this prime-boost antigenic response was based on (i) sustained levels of CD3+CD4+ with (ii) induction in effector memory CD3+CD4+ T-cells and (iii) higher frequency of CD3+CD8+ T-cells. This immune response in C57BL/6 was marked by (i) increased levels in the CD3+CD4+ T-cells, (ii) sustained levels of effector memory CD3+CD4+ T-cells, and (iii) enhanced frequency of effector memory CD3+CD8+ T-cells. In fact, previous data have reported that the LBSap vaccine presented a higher immunogenicity pattern displaying higher levels in the T-cells subsets (CD4+ and CD8+) [28], resulting in improved protection against *L. infantum* infection [24,31,53–55]. Additionally, the sponge implant model was able to further characterize the immune response after prime-boost protocol, providing different mechanisms associated with protection described in the LBSap vaccine in Swiss mice.

Functional analysis of the sponge microenvironment revealed that C57BL/6 mice induced a more prominent response after prime-boost protocol (group V/I) as compared to the other groups, presenting higher levels of cytokines with a mixed activation profile (IL- 6, TNF, IFN-γ, IL-10, and IL-17). In contrast, the cytokine analysis in Swiss mice revealed a prominent inflammatory response mediated mainly by IL-6, TNF, IFN-γ, and IL-17. Additionally, the BALB/c mice showed a similar inflammatory cytokine environment but confined to IL-6, TNF, and IFN-γ. It is important to emphasize that the immune response to an antigen can be determined by the environment in which it is found, being modulated by molecules such as cytokines [56,57]. In fact, the antigen in this microenvironment can trigger a different cytokine production that effectively drives the pattern of the immune response [47]. For example, the production of IFN-γ plays an essential role in inducing antiparasitic responses in macrophages, notably inducing the production of reactive oxygen species (ROS) and nitric oxide synthase (iNOS), essential for killing intracellular pathogens, such as *Leishmania* [58]. In addition, infection control in visceral leishmaniasis has been related to a Th1-type immune response, in which the pro-inflammatory cytokines IFN-γ /TNF must overcome the effects of the regulatory cytokine (IL-10), while susceptibility is related to a deficient pro-inflammatory

 doi:10.20944/preprints202410.1748.v1

response [53,55,59,60]. Some studies also report the importance of the cytokine IL-17 in controlling visceral leishmaniasis and developing vaccines against the disease [61]. According to Pitta *et al.* and Nascimento *et al.*, this cytokine plays an important protective role in human visceral leishmaniasis, complementing the protection conferred by inflammatory cytokines in a non-dependent manner or in synergy with IFN-γ, enhancing its action [62,63]. Similar to the data on cellular immune response described in Swiss mice, this strain presented a predominantly pro-inflammatory cytokine profile, reinforcing the applicability of this mice strain for immunogenicity analysis of vaccinal antigens. These data are supported by LBSap studies, demonstrating the presence of a pro-inflammatory cytokine profile (such as IL-6, TNF, IFN-γ, and an increased IFN-γ/IL-10 rate) associated with protection in visceral leishmaniasis [24,53,55,64].

5. Conclusions

The data from this study demonstrated that the implant using a polyester-polyurethane sponge in distinct mice strains provides a reliable *in vivo* model for immunogenicity studies applied to antigen testing for vaccine candidates. The data described the approach for immunogenicity testing using prime (vaccination) and boost (antigen inoculation at sponge implant), which was able to trigger the innate and adaptive immune responses. The selective stimulation in Ly+ neutrophils and CD11c+ dendritic cells reinforced the ability to assess the innate immune response. Moreover, the adaptive immune response was also induced as demonstrated by the induction in antigen-specific T-cells subsets, corroborating the application of this approach for immunogenicity testing of vaccine (antigens) candidates. In fact, the differential induction on T-cells subsets (CD4+ and CD8+) in the distinct mice strains validated the ability of this model to elicit antigen-specific central and effector memory immune responses. The Swiss mice presented the primary elements for immunogenicity analysis (induction of central memory based on T-cell cytoxicity and an intense inflammatory profile compose by IFN-γ, IL-17 and TNF). Although the BALB/c mice were not marked by a significant influence of adaptive immune response (T-cells memory), the microenvironment elicited in the sponge implant demonstrated a mixed pattern [with inflammatory (TNF, IL-6) and immunomodulatory (IL-10) cytokines]. The C57/BL6 mice showed immune biomarkers related to both Swiss and BALB/c mice with a prominent amount of CD4+ T-cells (including effector memory CD4+ T-cells) and an intense production of inflammatory cytokines (IL-17, IFN-γ, TNF, and IL-6) modulated by IL-10. The results highlighted how genetic background can influence the populations involved in the immune response and indicate that this model could be used to monitor the innate and adaptive immune responses of candidate vaccines. In this sense, these results could guide the choice of the most appropriate experimental model for testing biomolecules, given that the particularities of each mouse strain influenced the dynamics of the innate and adaptive immune responses.

Author Contributions: Conceptualization, Mariana Lanna, Lucilene Resende, Sandra Aparecida De Moura and Rodolfo Giunchetti; Data curation, Mariana Lanna; Formal analysis, Mariana Lanna, Lucilene Resende, Paula De Luca, Olindo Martins-Filho, Sandra Aparecida De Moura, Edelberto Dias, Érika Monteiro, Denise Silveira-Lemos and Rodolfo Giunchetti; Funding acquisition, Rodolfo Giunchetti; Investigation, Mariana Lanna, Lucilene Resende, Paula De Luca, Olindo Martins-Filho, Sandra Aparecida De Moura, Edelberto Dias, Érika Monteiro, Denise Silveira-Lemos and Rodolfo Giunchetti; Methodology, Mariana Lanna, Lucilene Resende, Paula De Luca, Alexandre Reis, Olindo Martins-Filho, Sandra Aparecida De Moura, Edelberto Dias, Érika Monteiro, Denise Silveira-Lemos and Rodolfo Giunchetti; Project administration, Rodolfo Giunchetti; Resources, Paula De Luca, Olindo Martins-Filho, Sandra Aparecida De Moura and Rodolfo Giunchetti; Supervision, Sandra Aparecida De Moura, Denise Silveira-Lemos and Rodolfo Giunchetti; Visualization, Mariana Lanna, Lucilene Resende, Wanessa Goes and Olindo Martins-Filho; Writing – original draft, Mariana Lanna and Lucilene Resende; Writing – review & editing, Mariana Lanna, Lucilene Resende, Paula De Luca, Wanessa Goes, Maykelin Zaldívar, André Costa, Walderez Dutra, Alexandre Reis, Olindo Martins-Filho, Kenneth Gollob, Sandra Aparecida De Moura, Edelberto Dias, Érika Monteiro, Denise Silveira-Lemos and Rodolfo Giunchetti. All authors have read and agreed to the published version of the manuscript.

Funding: This research received no external funding.

Institutional Review Board Statement: The animal study protocol was approved by the Ethics Committee of Federal University of Ouro Preto (protocol code 2011/14 and approval on July 6, 2014).

Data Availability Statement: All datasets generated for this study are included in the manuscript.

Acknowledgments: WOD: ABR, OAM-F, KJG, and RCG are grateful to CNPq for fellowships.

Conflicts of Interest: The authors declare no conflict of interest.

References

1. Andrade, S.P.; Machado, R.D.P.; Teixeira, A.S.; Belo, A. V.; Tarso, A.M.; Beraldo, W.T. Sponge-Induced Angiogenesis in Mice and the Pharmacological Reactivity of the Neovasculature Quantitated by a Fluorimetric Method. *Microvasc Res* **1997**, *54*, 253–261, doi:10.1006/MVRE.1997.2047.
2. Cassini-Vieira, P.; Deconte, S.R. amos; Tomiosso, T.C. arla; Campos, P.P. eixoto; Montenegro, C. de F.; Selistre-de-Araújo, H.S. obreiro; Barcelos, L.S.; Andrade, S.P. assos; Araújo, F. de A. DisBa-01 Inhibits Angiogenesis, Inflammation and Fibrogenesis of Sponge-Induced-Fibrovascular Tissue in Mice. *Toxicon* **2014**, *92*, 81–89, doi:10.1016/J.TOXICON.2014.10.007.
3. Rabelo, L.F.G.; Ferreira, B.A.; Deconte, S.R.; Tomiosso, T.C.; dos Santos, P.K.; Andrade, S.P.; Selistre de Araújo, H.S.; Araújo, F. de A. Alternagin-C, a Disintegrin-like Protein from Bothrops Alternatus Venom, Attenuates Inflammation and Angiogenesis and Stimulates Collagen Deposition of Sponge-Induced Fibrovascular Tissue in Mice. *Int J Biol Macromol* **2019**, *140*, 653–660, doi:10.1016/J.IJBIOMAC.2019.08.171.
4. Ferreira, B.A.; Moura, F.B.R. de; Cassimiro, I.S.; Londero, V.S.; Gonçalves, M. de M.; Lago, J.H.G.; Araújo, F. de A. Costic Acid, a Sesquiterpene from Nectandra Barbellata (Lauraceae), Attenuates Sponge Implant-Induced Inflammation, Angiogenesis and Collagen Deposition in Vivo. *Fitoterapia* **2024**, *175*, doi:10.1016/J.FITOTE.2024.105939.
5. Moura, S.A.L.; Lima, L.D.C.; Andrade, S.P.; Silva-Cunha Junior, A. Da; Órefice, R.L.; Ayres, E.; Da Silva, G.R. Local Drug Delivery System: Inhibition of Inflammatory Angiogenesis in a Murine Sponge Model by Dexamethasone-Loaded Polyurethane Implants. *J Pharm Sci* **2011**, *100*, 2886–2895, doi:10.1002/jps.22497.
6. Bailey, P.J. Sponge Implants as Models. *Methods Enzymol* **1988**, *162*, 327–334, doi:10.1016/0076-6879(88)62087-8.
7. Ferreira, M.A.N.D.; Barcelos, L.S.; Campos, P.P.; Vasconcelos, A.C.; Teixeira, M.M.; Andrade, S.P. Sponge-Induced Angiogenesis and Inflammation in PAF Receptor-Deficient Mice (PAFR-KO). *Br J Pharmacol* **2004**, *141*, 1185, doi:10.1038/SJ.BJP.0705731.
8. Belo, A. V.; Barcelos, L.S.; Ferreira, M.A.N.D.; Teixeira, M.M.; Andrade, S.P. Inhibition of Inflammatory Angiogenesis by Distant Subcutaneous Tumor in Mice. *Life Sci* **2004**, *74*, 2827–2837, doi:10.1016/J.LFS.2003.09.072.
9. Barcelos, L.S.; Talvani, A.; Teixeira, A.S.; Cassali, G.D.; Andrade, S.P.; Teixeira, M.M. Production and in Vivo Effects of Chemokines CXCL1-3/KC and CCL2/JE in a Model of Inflammatory Angiogenesis in Mice. *Inflammation Research* **2004**, *53*, 576–584, doi:10.1007/S00011-004-1299-4/METRICS.
10. De Oliveira, L.G.; Figueiredo, L.A.; Fernandes-Cunha, G.M.; De Miranda, M.B.; MacHado, L.A.; Da Silva, G.R.; De Moura, S.A.L. Methotrexate Locally Released from Poly(ε-Caprolactone) Implants: Inhibition of the Inflammatory Angiogenesis Response in a Murine Sponge Model and the Absence of Systemic Toxicity. *J Pharm Sci* **2015**, *104*, 3731–3742, doi:10.1002/JPS.24569.
11. Lanna, M.F.; Resende, L.A.; Aguiar-Soares, R.D. de O.; de Miranda, M.B.; de Mendonça, L.Z.; Melo Júnior, O.A. de O.; Mariano, R.M. da S.; Leite, J.C.; Silveira, P.; Corrêa-Oliveira, R.; et al. Kinetics of Phenotypic and Functional Changes in Mouse Models of Sponge Implants: Rational Selection to Optimize Protocols for Specific Biomolecules Screening Purposes. *Front Bioeng Biotechnol* **2020**, *8*, 538203, doi:10.3389/FBIOE.2020.538203/BIBTEX.
12. Xavier, D.O.; Amaral, L.S.; Gomes, M.A.; Rocha, M.A.; Campos, P.R.; Cota, B.D.C.V.; Tafuri, L.S.A.; Paiva, A.M.R.; Silva, J.H.; Andrade, S.P.; et al. Metformin Inhibits Inflammatory Angiogenesis in a Murine Sponge Model. *Biomedicine & Pharmacotherapy* **2010**, *64*, 220–225, doi:10.1016/J.BIOPHA.2009.08.004.
13. Agrawal, S.S.; Saraswati, S.; Mathur, R.; Pandey, M. Brucine, a Plant Derived Alkaloid Inhibits Inflammatory Angiogenesis in a Murine Sponge Model. *Biomedicine & Preventive Nutrition* **2011**, *1*, 180–185, doi:10.1016/J.BIONUT.2011.06.014.
14. Saraswati, S.; Pandey, M.; Mathur, R.; Agrawal, S.S. Boswellic Acid Inhibits Inflammatory Angiogenesis in a Murine Sponge Model. *Microvasc Res* **2011**, *82*, 263–268, doi:10.1016/J.MVR.2011.08.002.
15. Alhaider, A.A.; Gader, A.G.M.A.; Almeshal, N.; Saraswati, S. Camel Urine Inhibits Inflammatory Angiogenesis in Murine Sponge Implant Angiogenesis Model. *Biomedicine & Aging Pathology* **2014**, *4*, 9–16, doi:10.1016/J.BIOMAG.2013.10.003.
16. Alhaider, A.A.; Abdel Gader, A.G.M.; Almeshaal, N.; Saraswati, S. Camel Milk Inhibits Inflammatory Angiogenesis via Downregulation of Proangiogenic and Proinflammatory Cytokines in Mice. *APMIS* **2014**, *122*, 599–607, doi:10.1111/APM.12199.

17. Almeida, S.A.; Cardoso, C.C.; Orellano, L.A.; Reis, A.M.; Barcelos, L.S.; Andrade, S.P. Natriuretic Peptide Clearance Receptor Ligand (C-ANP4–23) Attenuates Angiogenesis in a Murine Sponge Implant Model. *Clin Exp Pharmacol Physiol* **2014**, *41*, 691–697, doi:10.1111/1440-1681.12251.
18. Cassini-Vieira, P.; Felipetto, M.; Prado, L.B.; Verano-Braga, T.; Andrade, S.P.; Santos, R.A.S.; Teixeira, M.M.; de Lima, M.E.; Pimenta, A.M.C.; Barcelos, L.S. Ts14 from Tityus Serrulatus Boosts Angiogenesis and Attenuates Inflammation and Collagen Deposition in Sponge-Induced Granulation Tissue in Mice. *Peptides (N.Y.)* **2017**, *98*, 63–69, doi:10.1016/J.PEPTIDES.2016.10.002.
19. Michel, A.F.R.M.; Melo, M.M.; Campos, P.P.; Oliveira, M.S.; Oliveira, F.A.S.; Cassali, G.D.; Ferraz, V.P.; Cota, B.B.; Andrade, S.P.; Souza-Fagundes, E.M. Evaluation of Anti-Inflammatory, Antiangiogenic and Antiproliferative Activities of Arrabidaea Chica Crude Extracts. *J Ethnopharmacol* **2015**, *165*, 29–38, doi:10.1016/J.JEP.2015.02.011.
20. Orellano, L.A.A.; Almeida, S.A.; Campos, P.P.; Andrade, S.P. Angiopreventive versus Angiopromoting Effects of Allopurinol in the Murine Sponge Model. *Microvasc Res* **2015**, *101*, 118–126, doi:10.1016/J.MVR.2015.07.003.
21. Ferreira, B.A.; Deconte, S.R.; de Moura, F.B.R.; Tomiosso, T.C.; Clissa, P.B.; Andrade, S.P.; Araújo, F. de A. Inflammation, Angiogenesis and Fibrogenesis Are Differentially Modulated by Distinct Domains of the Snake Venom Metalloproteinase Jararhagin. *Int J Biol Macromol* **2018**, *119*, 1179–1187, doi:10.1016/J.IJBIOMAC.2018.08.051.
22. Souza, R.A.C.; Ferreira, B.A.; Moura, F.B.R. de; Costa Silva, T. da; Cavalcanti, F.; Franca, E. de F.; Sousa, R.M.F. de; Febronio, J. de L.; Lago, J.H.G.; Araújo, F. de A.; et al. Dehydrodieugenol B and Hexane Extract from Endlicheria Paniculata Regulate Inflammation, Angiogenesis, and Collagen Deposition Induced by a Murine Sponge Model. *Fitoterapia* **2020**, *147*, 104767, doi:10.1016/J.FITOTE.2020.104767.
23. De Oliveira, L.G.; De Miranda, M.B.; De Moura, S.A.L.; Da Silva, G.R. Tacrolimus Delivered from Polymeric Implants Suppressed Inflammation and Angiogenesis in Vivo without Inducing Nephrotoxicity, Hepatotoxicity, and Myelosuppression. *J Drug Deliv Sci Technol* **2018**, *43*, 487–495, doi:10.1016/J.JDDST.2017.11.012.
24. De Mendonça, L.Z.; Resende, L.A.; Lanna, M.F.; Aguiar-Soares, R.D.D.O.; Roatt, B.M.; Castro, R.A.D.O.E.; Batista, M.A.; Silveira-Lemos, D.; Gomes, J.D.A.S.; Fujiwara, R.T.; et al. Multicomponent LBSap Vaccine Displays Immunological and Parasitological Profiles Similar to Those of Leish-Tec® and Leishmune® Vaccines against Visceral Leishmaniasis. *Parasit Vectors* **2016**, *9*, 1–12, doi:10.1186/S13071-016-1752-6/FIGURES/6.
25. Aguiar-Soares, R.D.D.O.; Roatt, B.M.; Ker, H.G.; Moreira, N.D.D.; Mathias, F.A.S.; Cardoso, J.M.D.O.; Gontijo, N.F.; Bruna-Romero, O.; Teixeira-Carvalho, A.; Martins-Filho, O.A.; et al. LBSapSal-Vaccinated Dogs Exhibit Increased Circulating T-Lymphocyte Subsets (CD4+ and CD8+) as Well as a Reduction of Parasitism after Challenge with Leishmania Infantum plus Salivary Gland of Lutzomyia Longipalpis. *Parasit Vectors* **2014**, *7*, doi:10.1186/1756-3305-7-61.
26. Aguiar-Soares, R.D. de O.; Roatt, B.M.; Mathias, F.A.S.; Reis, L.E.S.; Cardoso, J.M. de O.; de Brito, R.C.F.; Ker, H.G.; Corrêa-Oliveira, R.; Giunchetti, R.C.; Reis, A.B. Phase I and II Clinical Trial Comparing the LBSap, Leishmune®, and Leish-Tec® Vaccines against Canine Visceral Leishmaniasis. *Vaccines (Basel)* **2020**, *8*, 1–17, doi:10.3390/VACCINES8040690.
27. Giunchetti, R.C.; Corrêa-Oliveira, R.; Martins-Filho, O.A.; Teixeira-Carvalho, A.; Roatt, B.M.; Aguiar-Soares, R.D. de O.; Coura-Vital, W.; Abreu, R.T. de; Malaquias, L.C.C.; Gontijo, N.F.; et al. A Killed Leishmania Vaccine with Sand Fly Saliva Extract and Saponin Adjuvant Displays Immunogenicity in Dogs. *Vaccine* **2008**, *26*, 623–638, doi:10.1016/J.VACCINE.2007.11.057.
28. Giunchetti, R.C.; Corrêa-Oliveira, R.; Martins-Filho, O.A.; Teixeira-Carvalho, A.; Roatt, B.M.; de Oliveira Aguiar-Soares, R.D.; de Souza, J.V.; das Dores Moreira, N.; Malaquias, L.C.C.; Mota e Castro, L.L.; et al. Immunogenicity of a Killed Leishmania Vaccine with Saponin Adjuvant in Dogs. *Vaccine* **2007**, *25*, 7674, doi:10.1016/J.VACCINE.2007.08.009.
29. Resende, L.A.; Roatt, B.M.; Aguiar-Soares, R.D. de O.; Viana, K.F.; Mendonça, L.Z.; Lanna, M.F.; Silveira-Lemos, D.; Corrêa-Oliveira, R.; Martins-Filho, O.A.; Fujiwara, R.T.; et al. Cytokine and Nitric Oxide Patterns in Dogs Immunized with LBSap Vaccine, before and after Experimental Challenge with Leishmania Chagasi plus Saliva of Lutzomyia Longipalpis. *Vet Parasitol* **2013**, *198*, 371, doi:10.1016/J.VETPAR.2013.09.011.
30. Dores Moreira, N. Das; Vitoriano-Souza, J.; Roatt, B.M.; De Abreu Vieira, P.M.; Coura-Vital, W.; De Oliveira Cardoso, J.M.; Rezende, M.T.; Ker, H.G.; Giunchetti, R.C.; Carneiro, C.M.; et al. Clinical, Hematological and Biochemical Alterations in Hamster (Mesocricetus Auratus) Experimentally Infected with Leishmania Infantum through Different Routes of Inoculation. *Parasit Vectors* **2016**, *9*, doi:10.1186/S13071-016-1464-Y.
31. Roatt, B.M.; Aguiar-Soares, R.D. de O.; Vitoriano-Souza, J.; Coura-Vital, W.; Braga, S.L.; Corrêa-Oliveira, R.; Martins-Filho, O.A.; Teixeira-Carvalho, A.; de Lana, M.; Gontijo, N.F.; et al. Performance of LBSap Vaccine after Intradermal Challenge with L. Infantum and Saliva of Lu. Longipalpis: Immunogenicity and Parasitological Evaluation. *PLoS One* **2012**, *7*, e49780, doi:10.1371/JOURNAL.PONE.0049780.

32. Moreira, N. das D.; Giunchetti, R.C.; Carneiro, C.M.; Vitoriano-Souza, J.; Roatt, B.M.; Malaquias, L.C.C.; Corrêa-Oliveira, R.; Reis, A.B. Histological Study of Cell Migration in the Dermis of Hamsters after Immunisation with Two Different Vaccines against Visceral Leishmaniasis. *Vet Immunol Immunopathol* **2009**, *128*, 418–424, doi:10.1016/J.VETIMM.2008.11.030.
33. Resende, L.A.; Aguiar-Soares, R.D.D.O.; Gama-Ker, H.; Roatt, B.M.; De Mendonça, L.Z.; Alves, M.L.R.; Da Silveira-Lemos, D.; Corrêa-Oliveira, R.; Martins-Filho, O.A.; Araújo, M.S.S.; et al. Impact of LbSapSal Vaccine in Canine Immunological and Parasitological Features before and after Leishmania Chagasi-Challenge. *PLoS One* **2016**, *11*, doi:10.1371/JOURNAL.PONE.0161169.
34. Vitoriano-Souza, J.; Reis, A.B.; Moreira, N.D.; Giunchetti, R.C.; Correa-Oliveira, R.; Carneiro, C.M. Kinetics of Cell Migration to the Dermis and Hypodermis in Dogs Vaccinated with Antigenic Compounds of Leishmania Braziliensis plus Saponin. *Vaccine* **2008**, *26*, 3922, doi:10.1016/J.VACCINE.2008.04.084.
35. Vitoriano-Souza, J.; Moreira, N. das D.; Menezes-Souza, D.; Roatt, B.M.; De Oliveira Aguiar-Soares, R.D.; Siqueira-Mathias, F.A.; De Oliveira Cardoso, J.M.; Giunchetti, R.C.; De Sá, R.G.; Corrêa-Oliveira, R.; et al. Dogs Immunized with LBSap Vaccine Displayed High Levels of IL-12 and IL-10 Cytokines and CCL4, CCL5 and CXCL8 Chemokines in the Dermis. *Mol Immunol* **2013**, *56*, 540, doi:10.1016/J.MOLIMM.2013.05.231.
36. Luiza-Silva, M.; Campi-Azevedo, A.C.; Batista, M.A.; Martins, M.A.; Avelar, R.S.; Lemos, D.D.S.; Camacho, L.A.B.; Martins, R.D.M.; Maia, M.D.L.D.S.; Farias, R.H.G.; et al. Cytokine Signatures of Innate and Adaptive Immunity in 17DD Yellow Fever Vaccinated Children and Its Association With the Level of Neutralizing Antibody. *J Infect Dis* **2011**, *204*, 873–883, doi:10.1093/INFDIS/JIR439.
37. Andrade, S.P.; Fan, T.P.D.; Lewis, G.P. Quantitative In-Vivo Studies on Angiogenesis in a Rat Sponge Model. *Br J Exp Pathol* **1987**, *68*, 755–766.
38. Barcelos, L.S.; Coelho, A.M.; Russo, R.C.; Guabiraba, R.; Souza, A.L.S.; Bruno-Lima, G.; Proudfoot, A.E.I.; Andrade, S.P.; Teixeira, M.M. Role of the Chemokines CCL3/MIP-1α and CCL5/RANTES in Sponge-Induced Inflammatory Angiogenesis in Mice. *Microvasc Res* **2009**, *78*, 148–154, doi:10.1016/J.MVR.2009.04.009.
39. Mendes, J.B.; Campos, P.P.; Rocha, M.A.; Andrade, S.P. Cilostazol and Pentoxifylline Decrease Angiogenesis, Inflammation, and Fibrosis in Sponge-Induced Intraperitoneal Adhesion in Mice. *Life Sci* **2009**, *84*, 537–543, doi:10.1016/J.LFS.2009.01.023.
40. Guedes-da-Silva, F.H.; Shrestha, D.; Salles, B.C.; Figueiredo, V.P.; Lopes, L.R.; Dias, L.; Barcelos, L. da S.; Moura, S.; de Andrade, S.P.; Talvani, A. Trypanosoma Cruzi Antigens Induce Inflammatory Angiogenesis in a Mouse Subcutaneous Sponge Model. *Microvasc Res* **2015**, *97*, 130–136, doi:10.1016/J.MVR.2014.10.007.
41. Almeida, S.A. de; Orellano, L.A.A.; Pereira, L.X.; Viana, C.T.R.; Campos, P.P.; Andrade, S.P.; Ferreira, M.A.N.D. Murine Strain Differences in Inflammatory Angiogenesis of Internal Wound in Diabetes. *Biomedicine and Pharmacotherapy* **2017**, *86*, 715–724, doi:10.1016/J.BIOPHA.2016.11.146.
42. Pereira, L.X.; Viana, C.T.R.; Orellano, L.A.A.; Almeida, S.A.; Vasconcelos, A.C.; Goes, A. de M.; Birbrair, A.; Andrade, S.P.; Campos, P.P. Synthetic Matrix of Polyether-Polyurethane as a Biological Platform for Pancreatic Regeneration. *Life Sci* **2017**, *176*, 67–74, doi:10.1016/J.LFS.2017.03.015.
43. Scheuermann, K.; Orellano, L.A.A.; Viana, C.T.R.; Machado, C.T.; Lazari, M.G.T.; Capettini, L.S.A.; Andrade, S.P.; Campos, P.P. Amitriptyline Downregulates Chronic Inflammatory Response to Biomaterial in Mice. *Inflammation* **2021**, *44*, 580–591, doi:10.1007/S10753-020-01356-0/METRICS.
44. Orellano, L.A.A.; de Almeida, S.A.; Pereira, L.X.; Machado, C.T.; Viana, C.T.R.; Andrade, S.P.; Campos, P.P. Implant-Induced Inflammatory Angiogenesis Is up-Regulated in Obese Mice. *Microvasc Res* **2020**, *131*, 104014, doi:10.1016/J.MVR.2020.104014.
45. Bugya, Z.; Prechl, J.; Szénási, T.; Nemes, É.; Bácsi, A.; Koncz, G. Multiple Levels of Immunological Memory and Their Association with Vaccination. *Vaccines* **2021**, *Vol. 9, Page 174* 2021, *9*, 174, doi:10.3390/VACCINES9020174.
46. Giunchetti, R.C.; Silveira, P.; Resende, L.A.; Leite, J.C.; Melo-Júnior, O.A. de O.; Rodrigues-Alves, M.L.; Costa, L.M.; Lair, D.F.; Chaves, V.R.; Soares, I. dos S.; et al. Canine Visceral Leishmaniasis Biomarkers and Their Employment in Vaccines. *Vet Parasitol* **2019**, *271*, 87–97, doi:10.1016/J.VETPAR.2019.05.006.
47. Esser, M.T.; Marchese, R.D.; Kierstead, L.S.; Tussey, L.G.; Wang, F.; Chirmule, N.; Washabaugh, M.W. Memory T Cells and Vaccines. *Vaccine* **2003**, *21*, 419–430, doi:10.1016/S0264-410X(02)00407-3.
48. Rahimi, R.A.; Luster, A.D. Redefining Memory T Cell Subsets. *Trends Immunol* **2020**, *41*, 645–648, doi:10.1016/j.it.2020.06.003.
49. Sprent, J.; Surh, C.D. Generation and Maintenance of Memory T Cells. *Curr Opin Immunol* **2001**, *13*, 248–254, doi:10.1016/S0952-7915(00)00211-9.
50. Jameson, S.C.; Masopust, D. Understanding Subset Diversity in T Cell Memory. *Immunity* **2018**, *48*, 214–226, doi:10.1016/J.IMMUNI.2018.02.010.
51. Sallusto, F.; Geginat, J.; Lanzavecchia, A. Central Memory and Effector Memory T Cell Subsets: Function, Generation, and Maintenance. *Annu Rev Immunol* **2004**, *22*, 745–763, doi:10.1146/ANNUREV.IMMUNOL.22.012703.104702/CITE/REFWORKS.

52. Soon, M.S.F.; Engel, J.A.; Lee, H.J.; Haque, A. Development of Circulating CD4+ T-Cell Memory. *Immunol Cell Biol* **2019**, *97*, 617–624, doi:10.1111/IMCB.12272.
53. Leite, J.C.; Gonçalves, A.A.M.; de Oliveira, D.S.; Resende, L.A.; Boas, D.F.V.; Ribeiro, H.S.; Pereira, D.F.S.; da Silva, A.V.; Mariano, R.M. da S.; Reis, P.C.C.; et al. Transmission-Blocking Vaccines for Canine Visceral Leishmaniasis: New Progress and Yet New Challenges. *Vaccines 2023, Vol. 11, Page 1565* **2023**, *11*, 1565, doi:10.3390/VACCINES11101565.
54. Gonçalves, A.A.M.; Ribeiro, A.J.; Resende, C.A.A.; Couto, C.A.P.; Gandra, I.B.; dos Santos Barcelos, I.C.; da Silva, J.O.; Machado, J.M.; Silva, K.A.; Silva, L.S.; et al. Recombinant Multiepitope Proteins Expressed in Escherichia Coli Cells and Their Potential for Immunodiagnosis. *Microb Cell Fact* **2024**, *23*, doi:10.1186/S12934-024-02418-W.
55. Oliveira, D.S. de; Zaldívar, M.F.; Gonçalves, A.A.M.; Resende, L.A.; Mariano, R.M. da S.; Pereira, D.F.S.; Conrado, I. dos S.S.; Costa, M.A.F.; Lair, D.F.; Vilas-Boas, D.F.; et al. New Approaches to the Prevention of Visceral Leishmaniasis: A Review of Recent Patents of Potential Candidates for a Chimeric Protein Vaccine. *Vaccines* **2024**, *Vol. 12, Page 271* 2024, *12*, 271, doi:10.3390/VACCINES12030271.
56. Osero, B.O. ondo; Aruleba, R.T.; Brombacher, F.; Hurdayal, R. Unravelling the Unsolved Paradoxes of Cytokine Families in Host Resistance and Susceptibility to Leishmania Infection. *Cytokine X* **2020**, *2*, doi:10.1016/J.CYTOX.2020.100043.
57. Murtaugh, M.P.; Foss, D.L. Inflammatory Cytokines and Antigen Presenting Cell Activation. *Vet Immunol Immunopathol* **2002**, *87*, 109–121, doi:10.1016/S0165-2427(02)00042-9.
58. Michel, G.; Ferrua, B.; Munro, P.; Boyer, L.; Mathal, N.; Gillet, D.; Marty, P.; Lemichez, E. Immunoadjuvant Properties of the Rho Activating Factor CNF1 in Prophylactic and Curative Vaccination against Leishmania Infantum. *PLoS One* **2016**, *11*, e0156363, doi:10.1371/JOURNAL.PONE.0156363.
59. Singh, O.P.; Gidwani, K.; Kumar, R.; Nylén, S.; Jones, S.L.; Boelaert, M.; Sacks, D.; Sundar, S. Reassessment of Immune Correlates in Human Visceral Leishmaniasis as Defined by Cytokine Release in Whole Blood. *Clin Vaccine Immunol* **2012**, *19*, 961–966, doi:10.1128/CVI.00143-12.
60. Gonçalves, A.A.M.; Leite, J.C.; Resende, L.A.; Mariano, R.M. da S.; Silveira, P.; Melo-Júnior, O.A. de O.; Ribeiro, H.S.; de Oliveira, D.S.; Soares, D.F.; Santos, T.A.P.; et al. An Overview of Immunotherapeutic Approaches Against Canine Visceral Leishmaniasis: What Has Been Tested on Dogs and a New Perspective on Improving Treatment Efficacy. *Front Cell Infect Microbiol* **2019**, *9*, doi:10.3389/FCIMB.2019.00427.
61. Banerjee, A.; Bhattacharya, P.; Joshi, A.B.; Ismail, N.; Dey, R.; Nakhasi, H.L. Role of Pro-Inflammatory Cytokine IL-17 in Leishmania Pathogenesis and in Protective Immunity by Leishmania Vaccines. *Cell Immunol* **2016**, *309*, 37–41, doi:10.1016/J.CELLIMM.2016.07.004.
62. Pitta, M.G.R.; Romano, A.; Cabantous, S.; Henri, S.; Hammad, A.; Kouriba, B.; Argiro, L.; El Kheir, M.; Bucheton, B.; Mary, C.; et al. IL-17 and IL-22 Are Associated with Protection against Human Kala Azar Caused by Leishmania Donovani. *Journal of Clinical Investigation* **2009**, *119*, 2379–2387, doi:10.1172/JCI38813.
63. Nascimento, M.S.L.; Carregaro, V.; Lima-Júnior, D.S.; Costa, D.L.; Ryffel, B.; Duthie, M.S.; De Jesus, A.; De Almeida, R.P.; Da Silva, J.S. Interleukin 17A Acts Synergistically With Interferon γ to Promote Protection Against Leishmania Infantum Infection. *J Infect Dis* **2015**, *211*, 1015–1026, doi:10.1093/INFDIS/JIU531.
64. Giunchetti, R.C.; Silveira, P.; Resende, L.A.; Leite, J.C.; Melo-Júnior, O.A. de O.; Rodrigues-Alves, M.L.; Costa, L.M.; Lair, D.F.; Chaves, V.R.; Soares, I. dos S.; et al. Canine Visceral Leishmaniasis Biomarkers and Their Employment in Vaccines. *Vet Parasitol* **2019**, *271*, 87–97, doi:10.1016/J.VETPAR.2019.05.006.